A STATISTICAL STUDY OF THE VERTICAL STRUCTURE OF TRAVELING PLANETARY-SCALE WAVES

Raymond J. Deland and Keith W. Johnson [1]

New York University,[2] Bronx, N.Y.

ABSTRACT

The vertical structure of traveling planetary-scale waves is investigated using spherical harmonics of the geopotential field at levels from 1000 mb. to 10 mb., obtained from ESSA analyses. Fluctuations of the large-scale harmonics are analyzed using vector regression methods.

Westward-moving planetary-scale waves are shown to be present throughout the year at all the levels analyzed, with upward increasing amplitude in winter.

1. INTRODUCTION

Traveling planetary-scale waves (TPSW), of longitudinal wave numbers 1–3, have been described by Eliasen and Machenhauer [8], who analyzed spherical harmonics of the 500-mb. and 1000-mb. stream functions, and by Deland [6] and Deland and Lin [7] who analyzed spherical harmonics of the 500-mb. height. The waves have been shown to move westward on the average at speeds roughly half the speeds corresponding to non-divergent waves in a barotropic atmosphere (Rossby [18], Haurwitz [12]), i.e. at approximately the speeds corresponding to a barotropic atmosphere with a free upper surface (Rossby [18], Cressman [5]). Eliasen and Machenhauer [8], who analyzed the 500-mb. and 1000-mb. field for a 3-month winter period, have shown that the TPSW have somewhat smaller amplitude at 1000 mb. than at 500 mb. and approximately the same speed and phase at the two levels.

The vertical structure of the TPSW is of special interest because of its relation to the dynamics of these waves. Understanding their dynamics is essential if they are to be satisfactorily predicted by numerical models of the atmosphere. The recent "vorticity-equation" models used by the National Meteorological Center filter out the TPSW holding the planetary-scale waves stationary (Cressman [5], Deland and Lin [7]). The "planetary-wave" behavior of the new NMC primitive-equation model (Shuman et al. [20]) has not yet been analyzed.

The vertical structure of the TPSW and other transient components of the planetary-scale waves is also of importance in understanding the relations between large-scale motions in the troposphere and the stratosphere. There have been many synoptic studies of these relationships, of which one of the most relevant to the present study is that of Labitzke [14] who analyzed the relation of tropospheric blocking to sudden warmings in the stratosphere. Work based on Fourier and spherical harmonics has been recently reviewed by Sawyer [19] and Hare and Boville [11]. Boville [2] has shown that fluctuations of large-scale spherical harmonics of the geopotential field, similar to the TPSW, are in phase in the troposphere and stratosphere during January 1959, a period including a large-scale stratospheric warming. There have been some studies of the energetics of the stratospheric warming phenomenon in late winter by, among others, Muench [16] and Julian and Labitzke [13]. The question of the degree of interaction of the stratosphere with tropospheric planetary-scale waves is crucial in these studies. In a McGill University Ph.D. dissertation, Byron-Scott [3] has presented results of a numerical experiment, many aspects of which correspond remarkably well with the observations to be described in this paper.

We present in this paper the results of statistical computations of the fluctuations of spherical harmonics of the Northern Hemisphere geopotential field at levels from 1000 mb. to 10 mb., for a whole year. The stratospheric maps used were those of the Upper Air Branch, ESSA, for the 1964–65 IQSY period (Finger et al. [10]).

The spherical harmonics (1,2), (1,4), (2,3), and (2,5) only are analyzed because these largest-scale harmonics are those for which the westward-moving TPSW are well defined (Deland and Lin [7]). They are also the waves that are most likely to be propagated from the troposphere into the stratosphere (Charney and Drazin [4]), and the most likely to be adequately defined by the poor observational network at higher stratospheric levels.

We show evidence of the presence of TPSW during a large part of the year at all the levels analyzed, and

---

[1] Now with Weather Bureau, Environmental Science Services Administration, Silver Spring, Maryland.

[2] Contribution No. 59, Geophysical Sciences Laboratory, Department of Meteorology and Oceanography, New York University. This research has been supported by the Section on Atmospheric Sciences, National Science Foundation, NSF GA-362.

estimates of their amplitudes obtained by analyzing the fluctuations at each level, using the autoregression of day-to-day changes as previously used by Deland and Lin [7]. The presence of the waves is also shown by plotting them on polar diagrams in a few cases.

It is hypothesized that the TPSW behavior of a given harmonic at each level is due to the existence of a three-dimensional TPSW. The variation of amplitude and phase with height of the hypothetical three-dimensional TPSW is estimated from regressions of the harmonic at each level, except 500 mb., on the harmonic at 500 mb. This gives us a second method of estimating the variation of amplitude of the TPSW with height, the results of which can be compared with those from the autoregression procedure previously mentioned.

The particular method of harmonic decomposition used in this study is one of many possible ones, though some support for its use is provided by the theory of planetary motions of a barotropic atmosphere (Haurwitz [12], Platzman [17]). As used in this paper, the harmonic analysis is simply a convenient way of numerically representing the large-scale features of the geopotential field, with some separation of different horizontal scales.

2. DATA

We have computed odd (anti-symmetric about the Equator) spherical harmonics of the geopotential height of each constant pressure surface from Fourier harmonics along latitude circles from 87½°N. to 22½°N. at 2½° intervals. The Fourier harmonics were computed for us by NCAR, from grid point data on the 1977-point NMC grid.

The grid data were supplied from two sources. For each day (except for small gaps) of 1963, at 00 GMT, the National Meteorological Center, Suitland, Md., supplied data for the 1000-, 850-, 700-, 500-, 300-, 200-, 150-, and 100-mb. levels. For the IQSY period of July 1964 to June 1965, for each day (except some gaps) at 12 GMT, data were supplied by the Upper Air Branch, ESSA, for the 500-, 100-, 50-, 30- and 10-mb. levels. We thus have a year's data for all levels, a different year for the troposphere and stratosphere in general, with 2 years at 500 and 100 mb.

For each day, the spherical harmonic analysis expresses the geopotential field over the Northern Hemisphere at a particular pressure level as the sum of the zonal harmonics and the odd harmonics:

$$Z(\lambda, \varphi)=\sum_{n=0}^{N} Z_n P_n(\varphi)+\sum_{m=1}^{M}\sum_{n=m+1}^{M+L}(Z^m_{n_c}\cos m\lambda + Z^m_{n_s}\sin m\lambda)P^m_n(\varphi) \quad (1)$$

where the sum over n in the second expression on the right-hand side includes only values for which $n-m$ is odd. λ is longitude and φ is latitude. m is longitudinal wave-number. $Z_nP_n(\varphi)$ are the zonal harmonics, $P_n(\varphi)$ being the Legendre functions, which are not treated in this paper. For a particular tesseral harmonic (m, n) at a particular level on a particular day, $Z^m_{n_c}$ and $Z^m_{n_s}$ are fixed, and may be referred to as the "cosine" and "sine" components of the vector Z^m_n representing the particular harmonic. $Z^m_{n_c}$ and $Z^m_{n_s}$ define the amplitude and (longitudinal) phase of the harmonic. $P^m_n(\varphi)$ is the associated Legendre function. It is perhaps worth mentioning that the spherical harmonics (1,2) and (1,4) correspond roughly to the position and strength of the "polar" vortex (cyclonic at all levels in winter, anticyclonic at stratospheric levels in summer), so that the fluctuations of (1,2) that we analyze correspond to the wanderings of the circulation pole analyzed by LaSeur [15]. The harmonics (2,3) and (2,5) correspond to the bipolar pattern, with two troughs, which is a common synoptic feature of the winter stratosphere.

3. STATISTICAL METHODS

REGRESSIONS

The least squares best fit of (Y'_c, Y'_s) to $(\hat{Y}'_c, \hat{Y}'_s)$, where

$$(\hat{Y}'_c, \hat{Y}'_s)\equiv\begin{pmatrix} B_{11} & B_{12} \\ B_{21} & B_{22}\end{pmatrix}\begin{pmatrix} X'_c \\ X'_s\end{pmatrix} \quad (2)$$

(Ellison [9], Anderson [1]) was computed, where the primes refer to deviations from the sample mean. We will drop the primes from now on: the variables will be understood to be deviations from the sample mean. Correlation coefficients corresponding to the regressions were computed. These represent the square root of the fraction of the mean square magnitude of the (Y_c, Y_s) vector "explained" by regression on the (X_c, X_s) vector. The vector regression procedure was used both to analyze the fluctuations for the TPSW at each level, as was done for 500 mb. by Deland and Lin [7], and to correlate the fluctuations at different levels. In both cases the computations are done for the 12 separate months. The regression computations are illustrated in figure 1, which also illustrates the characteristic westward rotation of the deviation from the mean.

In the first, autoregression, procedure the regression computation, for a particular harmonic at a given level for a given month, finds the $[B]$ tensor that gives the best fit, over the month, of the observations to

$$\hat{\Delta}Z^m_{n_J}\equiv[B]\Delta Z^m_{n_{J-1}} \quad (3)$$

where $\Delta Z^m_{n_J}$ is the 24-hr. change in Z^m_n beginning on day J. This procedure is illustrated in figure 1 for the level "1". In the figure, $\Delta Z_{1_{J-1}}$ corresponds to $\Delta Z^m_{n_{J-1}}$ in equation (3), and so on. A more detailed discussion of the autoregression computation is given by Deland and Lin [7].

In the second procedure, also illustrated in figure 1, the regression computation gives the best fit, for a given harmonic in a given month, to

$$\hat{Z}^m_{n_J}(L_2)\equiv[B]Z^m_{n_J}(L_1) \quad (4)$$

where L_2 and L_1 represent the levels between which the regression is computed: in all calculations, both for troposphere and stratosphere, for this paper, L_1 is the 500-mb. level. In figure 1, $Z_{n_J}^m$ (L_2) and $Z_{n_J}^m$ (L_1) are represented by Z_2' and Z_1' respectively.

In both the autoregression and the vertical regression the angle of rotation corresponding to the tensor $[B]$ is calculated from

$$\begin{bmatrix} C & D \\ -D & C \end{bmatrix} \equiv \tfrac{1}{2}\begin{bmatrix} B_{11}+B_{22} & B_{12}-B_{21} \\ B_{21}-B_{12} & B_{11}+B_{22} \end{bmatrix}, \tag{5}$$

angle α being defined by

$$\sin \alpha = \frac{D}{\sqrt{C^2+D^2}}$$

$$\cos \alpha = \frac{C}{\sqrt{C^2+D^2}}.$$

For the autoregression, α (α_A in figure 1) is the average phase speed for the month, and for the vertical regression α (α_V in figure 1) is the average angle between the transient components at L_2 and those at 500 mb. If the correlation between the fluctuations at the two levels is due to the simultaneous presence of waves traveling at the same speed, the angle α in this case is a lag or phase difference between the traveling waves at the two levels. It might be preferable to estimate the phase change with height of a three-dimensional wave by a regression calculation that finds the best fit to a wave traveling at the same speed but possibly out of phase at the two levels. The simplest form for the corresponding vector regression is for four-dimensional vectors, with 12 B's to be found instead of four—the estimate being thus much more uncertain for a given sample size—and is far more complicated in general. We have therefore restricted ourselves to the simpler regression procedure.

For both regression procedures, the linear transformation corresponding to the regression can be considered to be made up of the "rotation plus stretching" part

$$\begin{bmatrix} C & D \\ -D & C \end{bmatrix}$$

and an irrotational "distortion." The "rotation plus stretching" part of the autoregression corresponds to a traveling wave, possibly uniformly growing or decreasing in amplitude during the month; in the vertical regression it corresponds to a variation of amplitude and an angular shift between the coherent fluctuations at different levels, such as would be due to the hypothetical three-dimensional TPSW. For convenience and brevity in showing to what extent the calculated regression fits the "rotation plus stretching" model, we have calculated in most cases a "rotation coefficient" R_r, defined as

$$R_r \equiv \left\{ \frac{2(C^2+D^2)}{B_{11}^2+B_{12}^2+B_{21}^2+B_{22}^2} \right\}^{1/2}. \tag{6}$$

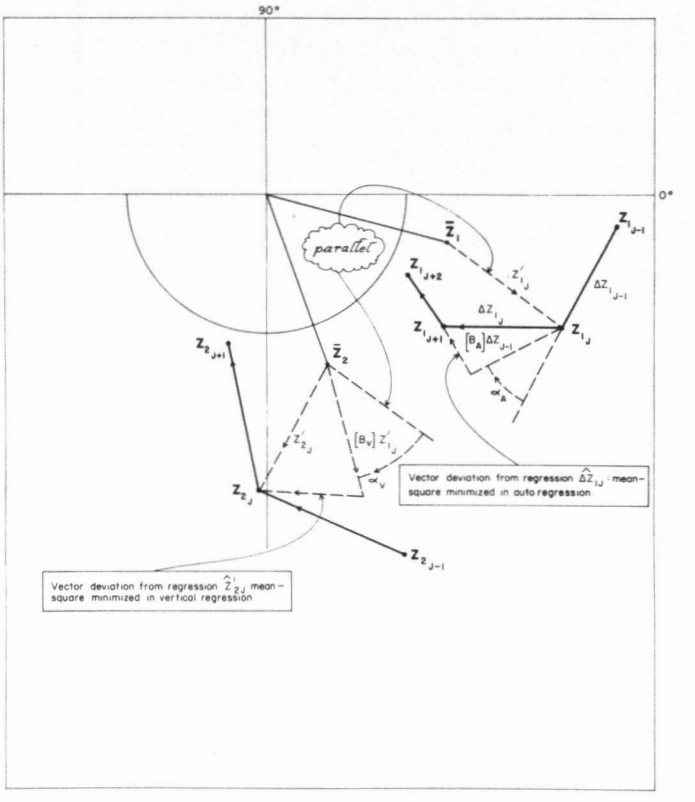

FIGURE 1.—Schematic diagram illustrating autoregression at level 1 and vertical regression of wave at level 2 on wave at level 1. The vector Z_{1_J} represents the amplitude and phase of a particular harmonic (m, n) at level 1 on day J, and $\overline{Z}_1$ represents the mean for a month.

This coefficient is 1 for a pure "rotation and stretching" regression tensor of the form

$$\begin{bmatrix} C & D \\ -D & C \end{bmatrix},$$

and 0.707 on the average if no "rotation and stretching" is present and the regression coefficients are uncorrelated.

It was found that in many of the vertical regressions for the stratospheric levels the coefficient R_r is systematically much less than 0.707. These values are not likely to be due to "noise," and in fact we will see later that the meaningful fluctuations can be disentangled from the average "distortion" even in these cases.

ESTIMATION OF AMPLITUDE OF TRAVELING WAVE

For autoregression, the expression (3) is the best estimate of that part of a change ΔZ_J that can be expressed as a linear function of the previous change ΔZ_{J-1}. Ignoring the small average "stretching" during the month, we estimate the change corresponding to rotation, that is due to the traveling wave (Deland and Lin [7]), as that part of ΔZ_J that corresponds to the orthogonal part of the tensor B, as

$$\Delta \hat{Z}_{R_J} \equiv \begin{bmatrix} C & D \\ -D & C \end{bmatrix} \begin{bmatrix} \Delta Z_{c_{J-1}} \\ \Delta Z_{s_{J-1}} \end{bmatrix}. \tag{7}$$

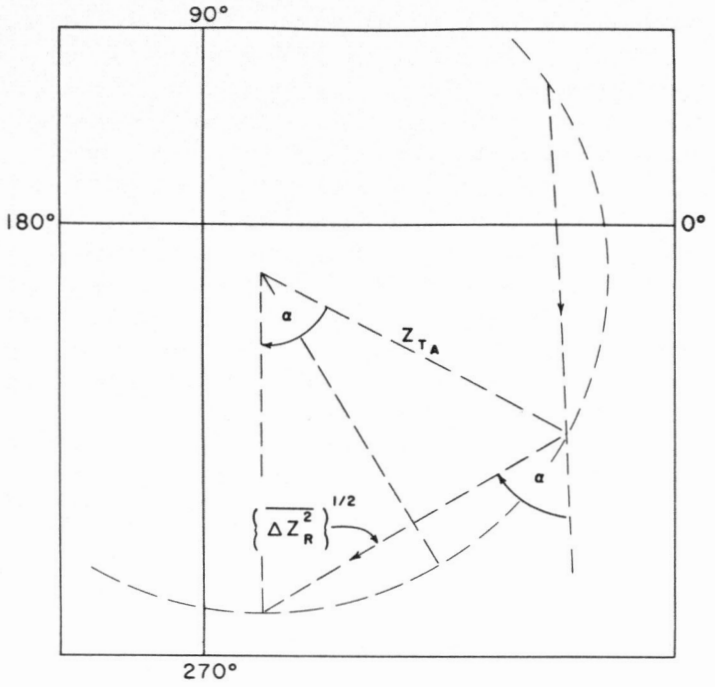

FIGURE 2.—Schematic diagram illustrating the calculation of the amplitude of the traveling wave from the "regression change" $\{\Delta Z_R^2\}^{1/2}$ and estimated angular speed α [equation (9)].

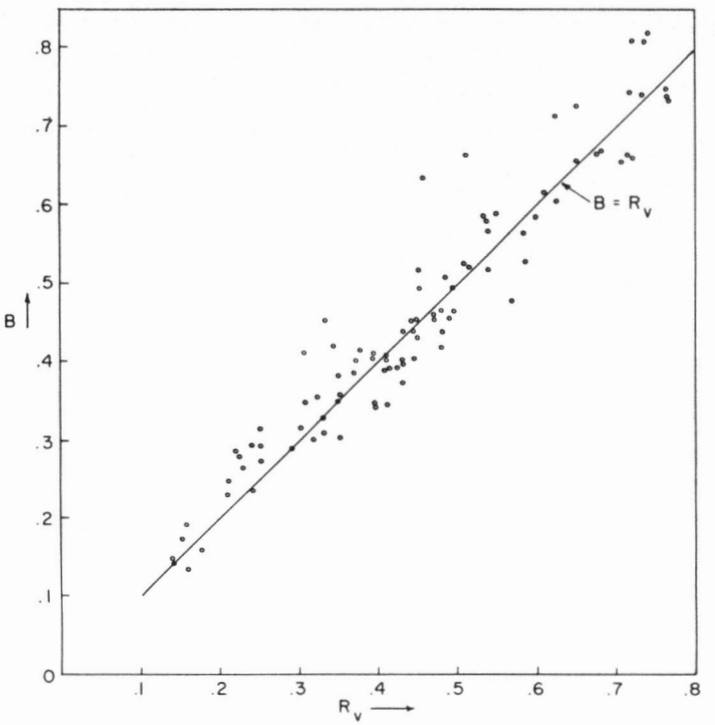

FIGURE 3.—Experimental verification of approximate equality of B [equation (12)] and the vector correlation coefficient R_v for autoregression. The values plotted are for an arbitrary sample of autoregression computations.

Squaring and averaging over the sample we get

$$\overline{\Delta Z_R^2} \equiv (C^2+D^2)(\overline{\Delta Z_{c_{J-1}}^2}+\overline{\Delta Z_{s_{J-1}}^2}). \tag{8}$$

The square root of the above expression is an estimate of the average change due to the traveling wave, and the amplitude of the wave causing the change is then obtained by trigonometry (see figure 2) as

$$Z_{T_A} \equiv \tfrac{1}{2}\{\overline{\Delta Z_R^2}\}^{1/2}/\sin\frac{\alpha}{2}. \tag{9}$$

From the vertical regressions we estimate the RMS magnitude of that part of the departure from the mean at each level (except 500 mb.) that is due to a "rotation and stretching" transformation of the value at 500 mb. As in the preceding paragraph, the part of $Z_J(L_2)$ that is a "rotation and stretching" transformation of $Z_J(L_1)$ where L_1 is 500 mb., is given by

$$\hat{Z}_J(L_2) \equiv \begin{bmatrix} C & D \\ -D & C \end{bmatrix} \begin{bmatrix} Z_{c_J}(L_1) \\ Z_{s_J}(L_1) \end{bmatrix}. \tag{10}$$

The root mean square magnitude of $\hat{Z}(L_2)$ is given, as before, by

$$Z_r \equiv \{(C^2+D^2)\,(\overline{Z_{c_J}^2(L_1)}+\overline{Z_{s_J}^2(L_1)})\}^{1/2}. \tag{11}$$

For the interpretation of the vertical regressions in terms of amplitude we need an approximate relationship between the regression coefficients and the vector correlation coefficient. It is well known, for ordinary scalar regression, that regression coefficients "regress" toward zero with decreasing correlation due to added noise, in approximate proportion to the correlation coefficient. This relationship is apparent in the algebraic formulas for the regression and correlation coefficients, for the vector regression used here as well as for the simple scalar regression. It is to be expected from consideration of the formulas and from simple statistical models, that the following approximation should be valid for the case when the variances of the predictor and predictand vectors are the same:

$$R_v \approx B \equiv \{\tfrac{1}{2}(B_{11}^2+B_{12}^2+B_{21}^2+B_{22}^2)\}^{1/2} \tag{12}$$

where R_v is the vector correlation coefficient. This relationship was tested by plotting R_v against B for a considerable number of the autoregression computations, as shown in figure 3. It is apparent from the figure that the two statistics can be considered to be approximately equal.

In order to interpret the results of the vertical regressions in terms of the hypothetical three-dimensional traveling waves described in the introduction, we make use of some of the results from the autoregression analysis. It will be seen in the next section that on the average the proportion of the fluctuations due to the TPSW is greater at 500 mb. than at other levels. If the 500-mb. fluctuations were purely TPSW, the best estimate of the amplitude of the TPSW from the vertical regression on 500 mb. would be the Z_r defined above. If, on the other hand, the TPSW were obscured by noise at both levels in proportion to the magnitude of the TPSW at each level, it follows

284-383 O - 68 - 3

from the approximation (12) that the best estimate of the magnitude of the TPSW would be the Z_r divided by the correlation coefficient. Since the actual situation is somewhere between these two statistical models, we compromise by dividing Z_r by the square root of the correlation coefficient, i.e. we define

$$Z_{T_V} \equiv \frac{(C^2+D^2)^{1/2}}{R_v^{1/2}} \overline{(Z_{c_J}^2(L_1)+Z_{s_J}^2(L_1))}^{1/2}. \qquad (13)$$

4. RESULTS OF STATISTICAL COMPUTATIONS

Because the number of statistics computed is large, we present them in graphical form in figures 4, 5, 8, and 9. We do not show all the individual regression coefficients, but only the vector correlation coefficient R_v, the "rotational coefficient" R_r [equation (6)], and the angle of rotation corresponding to the regression tensor.

AUTOREGRESSION

The autoregression results for each month are shown for the "tropospheric" (1000–100 mb.) and "stratospheric" (500–10 mb.) computations in figures 4 and 5, respectively. R_v and R_r are plotted together on the same figure to make comparison and discussion easier. The angle of rotation as plotted corresponds to phase-speed of the TPSW, in the sense of westward speeds being counted as positive. The phase-speeds for the longitudinal wave-number 2 [spherical harmonics (2,3) and (2,5)] are twice the wave-speeds in degrees of longitude per day. We have also plotted on these figures, for comparison, the "summer" (June and July 1962) and "winter" (January and February 1962) average phase-speeds calculated by Deland and Lin [7] for these waves at 500 mb.

Positive, that is westward, phase-speeds, consistent from month to month, and values of the rotation coefficient R_r close to 1 are obtained for all four harmonics in nearly all months at 500 and 300 mb. The waves appear to be a little better defined, on the basis of higher values of R_v and R_r and more consistent phase-speed α, at 500 mb. than at 300 mb.

In the case of the largest-scale harmonic (1,2), constancy of phase-speed from level to level indicates the existence of three-dimensional TPSW extending through all of the levels considered here, from 1000 mb. to 10 mb., almost throughout the year. The only exceptions are for 1000 mb. in February and 850 mb. in November, and some months at 100 mb.

For the other harmonics, the results are less simple. At lower levels, during 1963 (fig. 4) we see that the TPSW appear well defined, and vertically consistent in June and July down to 1000 mb. in all cases. In other months the results are erratic: the TPSW are apparent down to 1000 mb. in some months for each harmonic. No additional seasonal pattern is apparent in the results for the troposphere.

Although little if any seasonal variation is apparent in R_v and R_r for the tropospheric levels there is considerable fluctuation from month to month. The fact that the fluctuations of R_v and R_r are well correlated, as can be seen by inspection of figure 4, is additional evidence that the regression results and the calculated correlations in particular are mainly due to the presence of the TPSW.

In the stratosphere, for July 1964–June 1965 (fig. 5), there is a strong seasonal variation of the apparent incidence of TPSW for all four harmonics, as deduced from consistency of angle of rotation and the values of R_v and R_r. The TPSW appear relatively well defined in winter, from November to March. From June to October the correlations are rather low and the rotation angles highly erratic at and above 100 mb. even for (1,2) (in this respect differing somewhat from the comparable results for 100 mb. in 1963—figure 4). There is a moderate correlation of month-to-month values of R_v and R_r in the stratosphere, with some conspicuous exceptions such as (2,3) and (2,5) in January.

The relatively large seasonal variation of the average speeds of the TPSW, already discussed by Deland and Lin [7] is borne out in these more detailed results. Superimposed on the seasonal variation of phase-speeds are large fluctuations from month to month. These fluctuations have not yet been studied in detail: it is planned to treat them in a later report.

Polar diagrams for (1,2) at 500 mb. and 30 mb. for July and January are plotted in figures 6 and 7. The characteristic rotation corresponding to the presence of the TPSW is apparent at both levels in both months. It is also apparent that the fluctuations are approximately in phase at the two levels, as will be demonstrated statistically in the following section. This behavior of the fluctuations is in conspicuous contrast to the behavior of the mean waves, which are roughly opposite in phase in the troposphere and stratosphere. The contrast is well illustrated in figures 6 and 7.

The relationship of these results to the mean fields on which the waves are superimposed is of interest. The pole of circulation, in the sense of LaSeur [15], will describe clockwise roughly circular paths as the wave moves westward. This is true even in summer when the vortex at 30 mb. is anticyclonic. Comparison of the amplitude of these waves with the strength of the anticyclonic vortex at 30 mb. in summer (see Hare and Boville [11]) shows that the perturbations are relatively very small and quite unnoticeable on a hemispheric map. The corresponding motions of the cyclonic vortex in winter are subjectively apparent at times.

VERTICAL REGRESSIONS

The correlation coefficient R_v, rotation coefficient R_r, and rotation angle α for the vertical regressions are presented graphically in figures 8 and 9. The rotation coefficient R_r has been calculated for the "stratosphere" regressions only. The angles of rotation obtained from

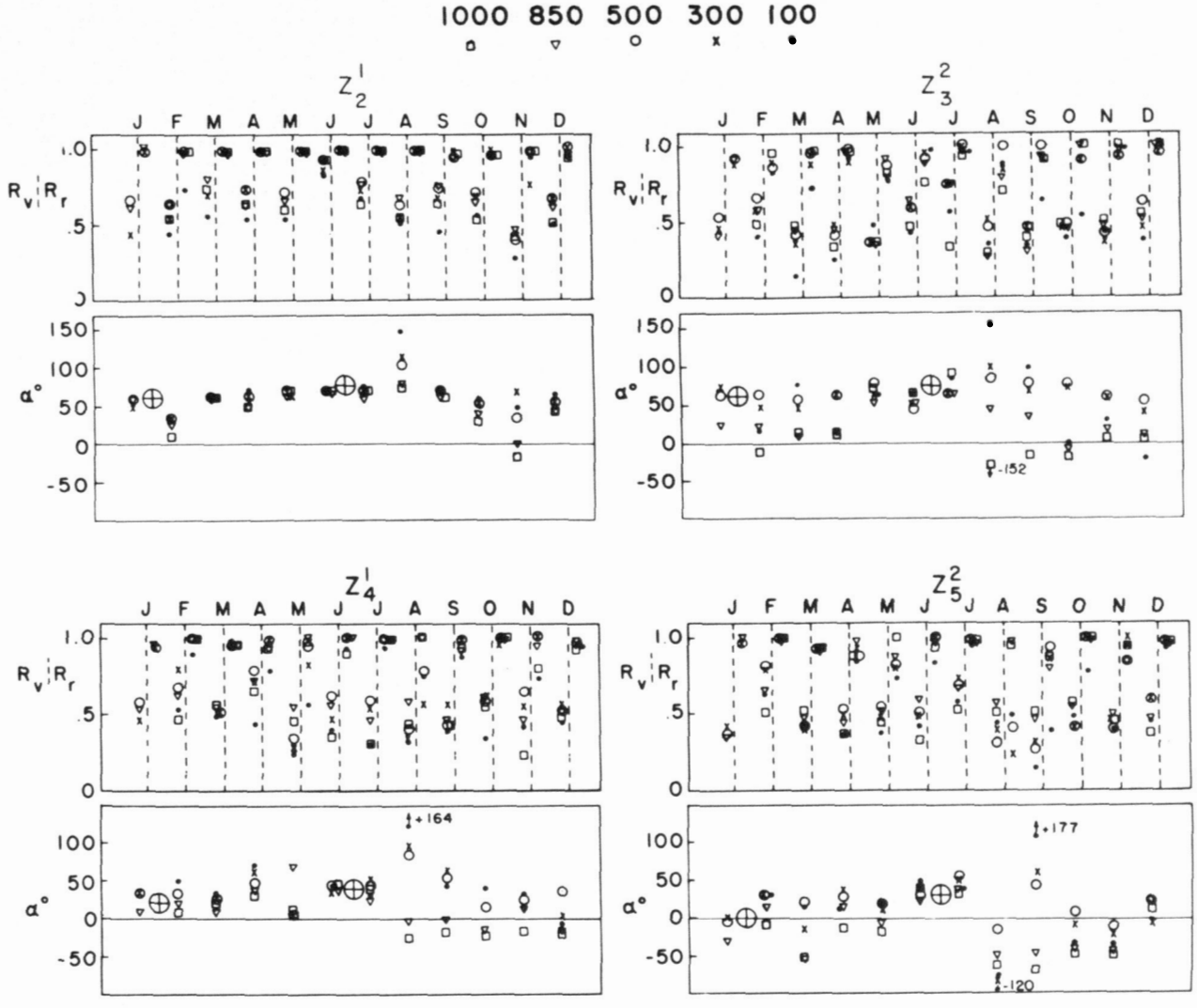

FIGURE 4.—Autoregression results, 1000 mb. to 100 mb., January–December 1963. In the upper part of each section, under each month the vector correlation R_v is plotted on the left and the rotation coefficient R_r [equation (7)] is plotted on the right. ⊕ denotes 2-month means from Deland and Lin [7].

the vertical regressions correspond to a phase-shift of the hypothetical three-dimensional TPSW with height, as is illustrated in figure 1.

The vertical correlations behave essentially as would be expected from the autoregression results. In the troposphere we observe high correlations throughout the year, even down to 1000 mb., especially for (1,2). The vertical and autoregression statistics for the troposphere are well correlated from month-to-month in the troposphere, providing convincing evidence that the vertical correlation is due mainly to similar fluctuations that fall into a regular pattern at each level and thus contribute to the autocorrelation.

The vertical correlations between 500 mb. and stratospheric level do not show the seasonal variation seen in the autoregression statistics. Likewise the month-to-month correlation of vertical and autoregression statistics, observed in the troposphere, is not apparent in the stratospheric statistics, though some of the variations seem to match for the two regression calculations. Since the autoregression analysis indicates that the three-dimensional TPSW extend up into the stratosphere significantly more in winter than in summer, the lack of seasonal variation of the vertical correlations is surprising. The discrepancy can be explained, however, by considering the day-to-day fluctuations.

Let us consider the vertical and autoregression for the stratosphere for July and January, and day-to-day fluctuations at 500 and 30 mb. as shown in figures 6 and 7. The auto-correlation and rotation coefficients at 500 mb. are similar and quite high during both months, but at 30 mb. the correlations are considerably lower during July than in January, indicating that the TPSW is well defined at 30 mb. in January but not in July. But the

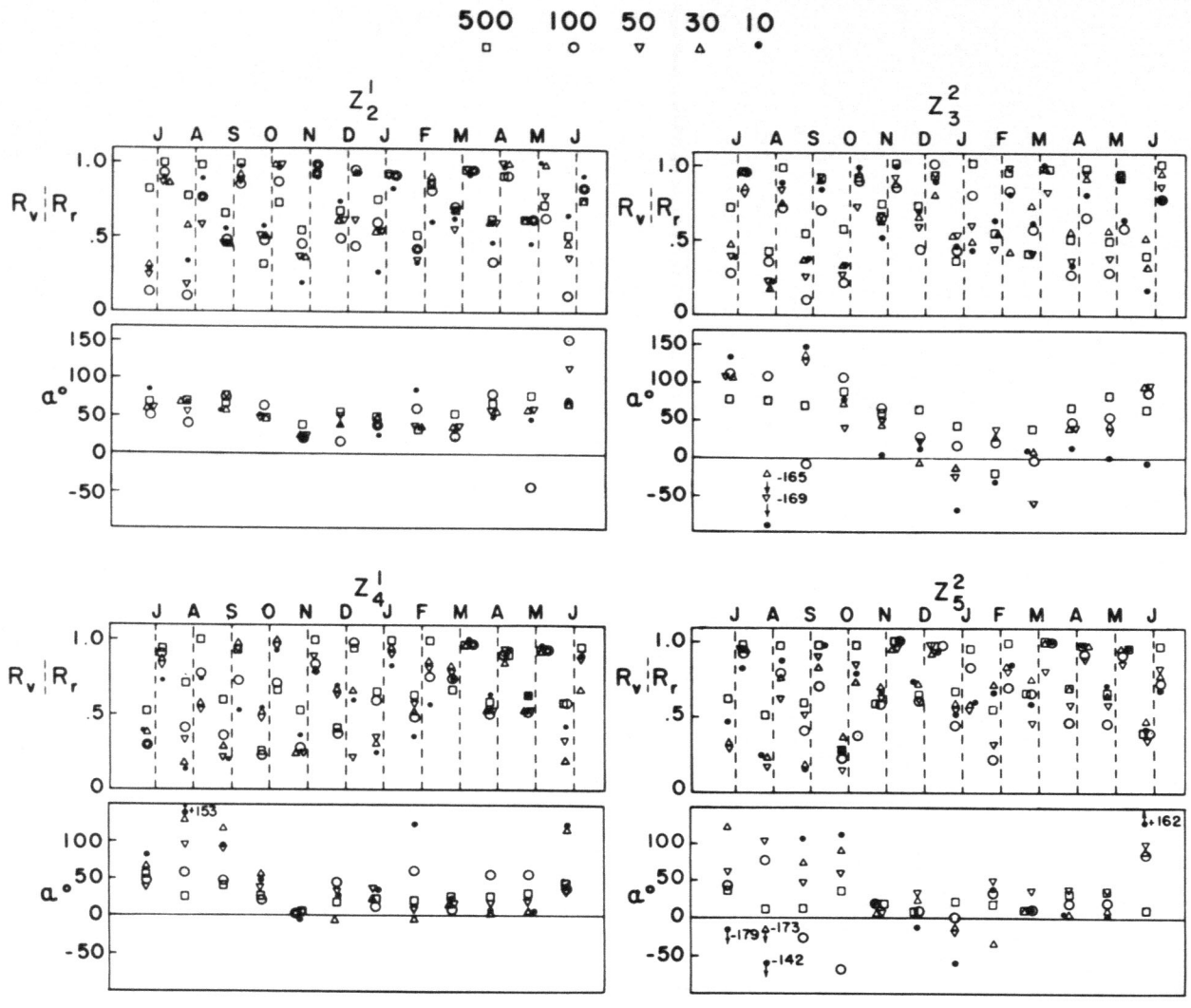

FIGURE 5.—Autoregression results, 500–10 mb., July 1964–June 1965. Otherwise as in figure 3.

vertical correlation of the 30 mb. and 500 mb. harmonics is considerably less in January than in July. Examination of the day-to-day fluctuations at 30 mb. and 500 mb. in July shows that at both levels the fluctuations are of the TPSW kind, but less organized at 30 mb. than at 500 mb. At both levels the fluctuations were such that the harmonic at no time departed far from the mean for the month. The result is that the TPSW-type fluctuations at both levels cause departures from the means that are in phase at the two levels, thus contributing to the vertical correlation. In January we again see the characteristic TPSW-type rotation around the mean at 500 mb., but at 30 mb. the TPSW-type fluctuation appears to be around a shifting center that itself moves roughly once around the mean during the month. As a consequence the 30-mb. departure from the mean, which is largely due to non-TPSW fluctuations, is out-of-phase with the 500-mb. departure from the mean during part of the month, thus reducing the vertical correlation. Large slow fluctuations in the stratosphere are conspicuous during the other winter months also, and appear sufficient to explain the discrepancy between the vertical and autoregression results.

After the vertical regressions were calculated it appeared that it would have been better to correlate the day-to-day changes, as was done in the autoregression, because the results would be relatively insensitive to the slow fluctuations of the "quasi-stationary" component discussed above. The probable return for the extra computation did not, however, appear to justify recalculation.

For all four harmonics, in most months, we find almost monotonically increasing westward shift with increasing height through the entire height range up to 10 mb. The variation of phase-shift with height is mostly rather small through the troposphere, of the order of 10° or 20°, and considerably larger, 50° or more, from 500 mb. to 10 mb., the largest variation being from 30 to 10 mb. As already discussed in the Introduction, we can consider these phase-shifts to represent a westward tilt with increasing height of the hypothetical three-dimensional

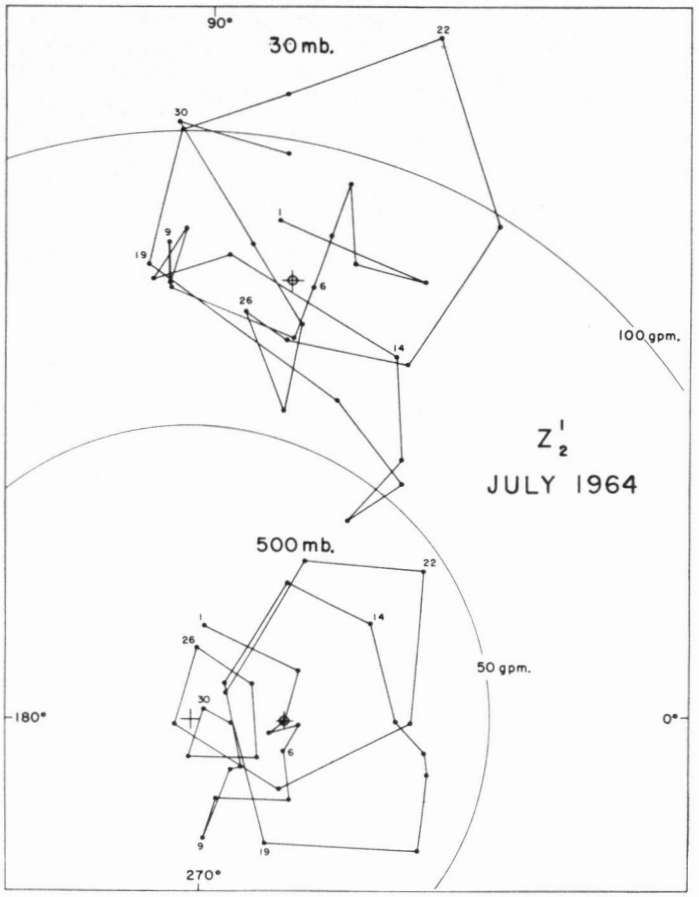

FIGURE 6.—Polar representation of the harmonic Z_2^1 at 500 mb. and 30 mb. on each day of July 1964. ⊕ denotes the mean amplitude and phase of the wave during the month.

TPSW. There is no conspicuous seasonal pattern in the vertical phase-shifts up to 100 mb. The stratospheric phase-shifts for all four harmonics show less westward shift with increasing height in the spring than at other seasons, except for the eastward tilt of (1,2) in January.

The January (1,2) case shown in figure 7 happens to be one for which the computed phase-shifts are small (and eastward in the stratosphere), and in fact little phase-difference between 500 and 30 mb. would be expected from the figure. In cases where the computed phase-differences are large and westward, e.g. (1,2) in July, the average phase-differences are clearly evident on the polar diagrams if the departures from the mean are compared for the two levels.

AMPLITUDE OF TPSW

The amplitude of the waves at levels from 1000 mb. to 100 mb. have been estimated from the autoregression for the months of January, March, and June of 1963. These amplitudes are shown in table 1. Because the estimated amplitudes show considerable variability due to their dependence on the angle of rotation α [equation (9)], the root-mean-square amplitude of the regression day-to-day fluctuation $(\Delta Z_r^2)^{1/2}$ [equation (9)] is also tabulated.

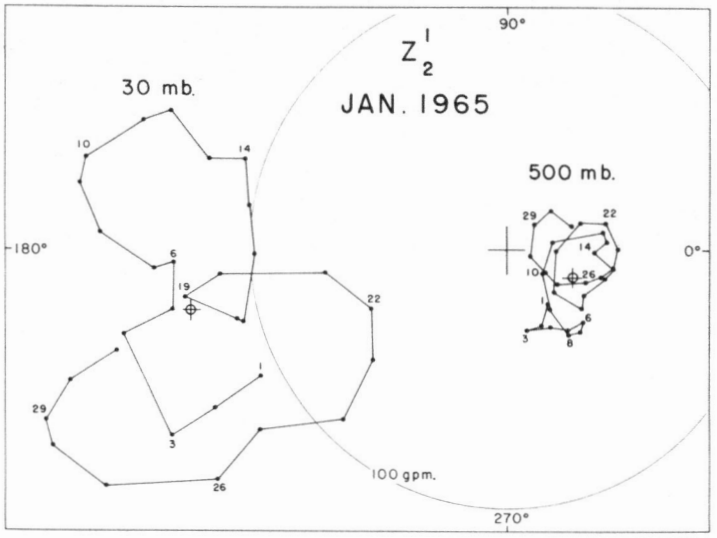

FIGURE 7.—Z_2^1 at 500 mb. and 30 mb. during January 1965. Otherwise as in figure 5.

TABLE 1.—*Amplitude of mean traveling waves from autoregression* Z_{T_A} *[equation (9)], and of the mean change* $(\Delta Z_R^2)^{1/2}$ *(see text, equation [8]). Bracketed values are unreliable due to relatively uncertain estimates of wave-speed.*

Level (mb.)	January,		March,		June 1963, 1000–100 mb.	
	Z_{T_A}	$(\Delta Z_R^2)^{1/2}$	Z_{T_A}	$(\Delta Z_R^2)^{1/2}$	Z_{T_A}	$(\Delta Z_R^2)^{1/2}$
			Wave (1, 2)			
1000			14.3	13.7	19.1	21.3
850	9.7	9.8	15.5	14.9	18.9	21.0
700	10.9	10.5	16.3	16.2	20.5	22.8
500	12.8	12.4	17.4	18.0	21.8	24.3
300	11.8	9.6	19.2	19.0	19.0	30.8
200	8.7	9.0	19.0	17.8	24.2	34.7
150			18.9	17.1	23.5	25.9
100			17.4	17.2	20.3	24.4
			Wave (1, 4)			
1000			28.1	8.4	5.2	3.7
850	73.2	8.6	48.4	7.7	8.5	5.3
700	34.8	10.0	35.9	8.0	8.7	6.0
500	21.8	10.8	21.3	8.9	10.0	7.3
300	19.2	11.0	24.0	11.9	11.5	6.6
200	17.4	10.2	25.7	9.7	13.0	6.8
150			23.6	9.3	6.5	5.3
100			14.3	11.2	6.7	4.9
			Wave (2, 3)			
1000			25.5	5.7	4.6	4.9
850	13.3	5.0	(42.7)	5.3	6.6	5.6
700	8.3	6.2	9.4	5.2	7.4	6.0
500	8.0	8.2	5.9	5.4	8.8	6.4
300	7.0	8.9	7.1	5.5	10.0	7.9
200	3.1	(4.1)	17.4	4.7	11.4	8.2
150			(197.3)	3.6	7.4	5.2
100			(194.9)	1.9	5.4	5.6
			Wave (2, 5)			
1000			8.0	7.4	5.0	3.0
850	10.4	5.5	6.4	5.7	12.2	3.9
700	9.5	5.0	8.9	3.7	10.8	4.0
500	(54.6)	6.2	12.5	4.0	9.8	5.1
300	(874.3)	9.0	(22.8)	6.2	10.8	6.6
200	8.7	4.8	12.4	7.5	11.8	7.6
150			17.8	6.0	9.0	6.4
100			(19.5)	5.4	5.9	4.7

On the average the results show a moderate increase in amplitude, by 50 or 100 percent, from 1000 mb. up to 300 mb., with a decrease from 300 to 100 mb. No systematic departure from this pattern either by month or harmonic is apparent, but the sample is too small for definite conclusions to be drawn about this.

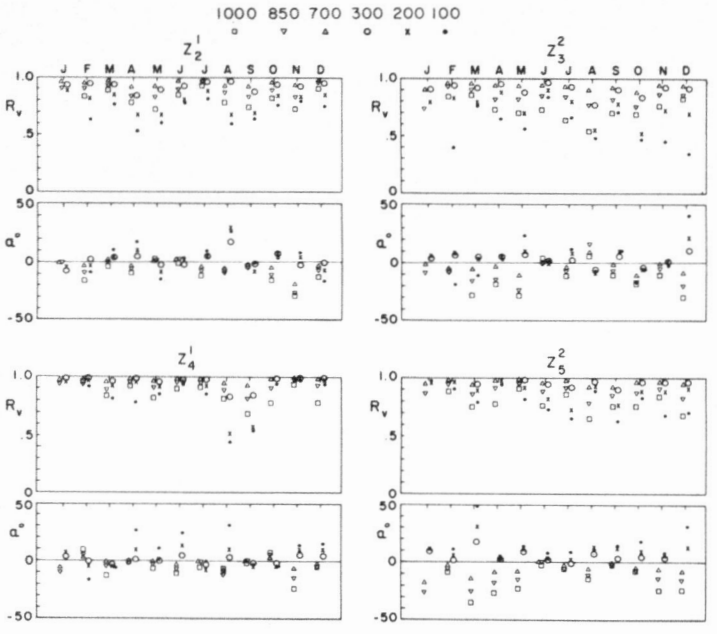

FIGURE 8.—Vertical regression results, 1000 mb.–100 mb. vs. 500 mb., January–December 1963; R_v and α only. Under each month values for levels above 500 mb. are plotted on the right, levels below 500 mb. on the left.

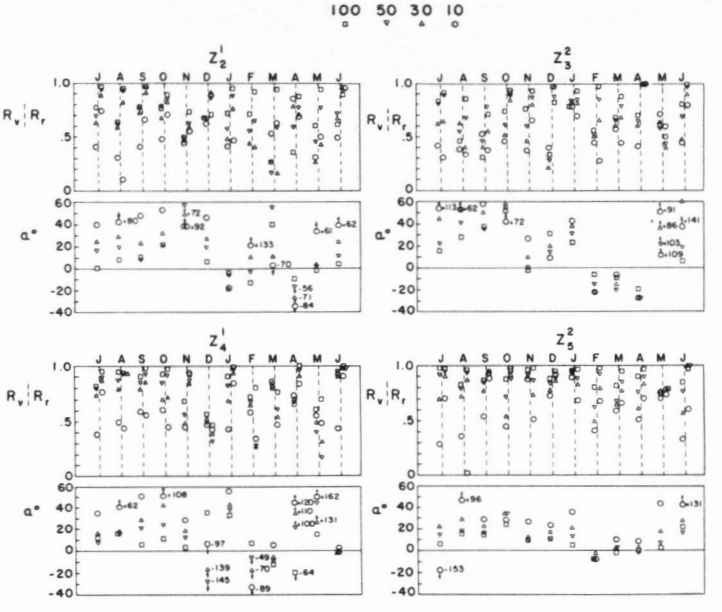

FIGURE 9.—Vertical regression results, 500 mb.–10 mb., July 1964–June 1965 R_v and R_r both plotted, as in figure 3.

The amplitude of the TPSW at 500, 100, 50, 30, and 10 mb. has been estimated from the vertical and autoregressions, as described in section 3, for all 12 months from July 1964 to June 1965. The estimated amplitudes of the TPSW at 500 mb. and the ratios of the amplitudes at each level to that at 500 mb. have been plotted in figure 10. Amplitudes at 500 mb. for January, March, and June 1963 (table 1) are also plotted in figure 10. Because of the sensitivity of the autoregression estimate to angle of rotation, we have omitted autoregression estimates of the amplitude ratios for which the variation of rotation angle with height would by itself cause the ratio of the estimated amplitude to the 500-mb. value to be less than 1:2 or more than 2:1.

The 500-mb. amplitude for (1,2) is approximately constant at 10 to 15 gpm. throughout the year. There is some seasonal variation in the estimated amplitudes of the other components, with greater amplitudes being observed in winter. This seasonal variation is in accordance with the variation of the speed of the waves (figures 4 and 5 and equation [9]), so that the average daily change due to the waves $(\overline{\Delta Z_R^2})^{1/2}$ is approximately constant throughout the year.

The ratios of amplitudes in the stratosphere to 500-mb. amplitudes show a strong seasonal variation, amplitude increasing upward in winter, approximately from November to April, and decreasing with height in summer. This seasonal variation is also clearly evident in the polar diagrams of (1,2) for July and January, figures 6 and 7. The amplitude ratios shown in figure 10 vary erratically from month-to-month, especially in winter, partly because of the large slow variations that have already been discussed. It appears, however, from the polar diagrams for different months (not shown, except for the few in figures 6 and 7) that the upward increase in amplitude of correlated fluctuations varies considerably from month to month and also during shorter periods than a month.

The upward increase in amplitude in winter is greatest for (1,2). This is consistent with theoretical results such as those of Charney and Drazin [4]. It is difficult, however, to estimate to what extent it is due to the fact that current observational networks and analysis procedures filter out smaller-scale fluctuations in the stratosphere.

5. CONCLUSION

The three-dimensional westward traveling planetary-scale wave model suggested in the Introduction is well supported, in general, by the statistical results and also by subjective comparison of the polar representations of the waves at different levels. There are considerable variations from month to month in the proportion of the total fluctuations that can be ascribed to the TPSW. In the troposphere the waves are fairly constant in amplitude throughout the year; in the stratosphere they increase upward strongly in winter but in summer are approximately constant with height. Conspicuous stratospheric activity in the autumn and spring appears to be largely due to the small amplitudes of the "mean" waves and weak zonal winds at these times rather than to stronger influence of tropospheric disturbances. Our results do not agree with the conclusion of Charney and Drazin [4] that the strong westerlies of the winter time stratospheric vortex inhibit the response of the stratosphere to changes in the troposphere. This is not surprising considering the approximations and simplifying assumptions they had to make.

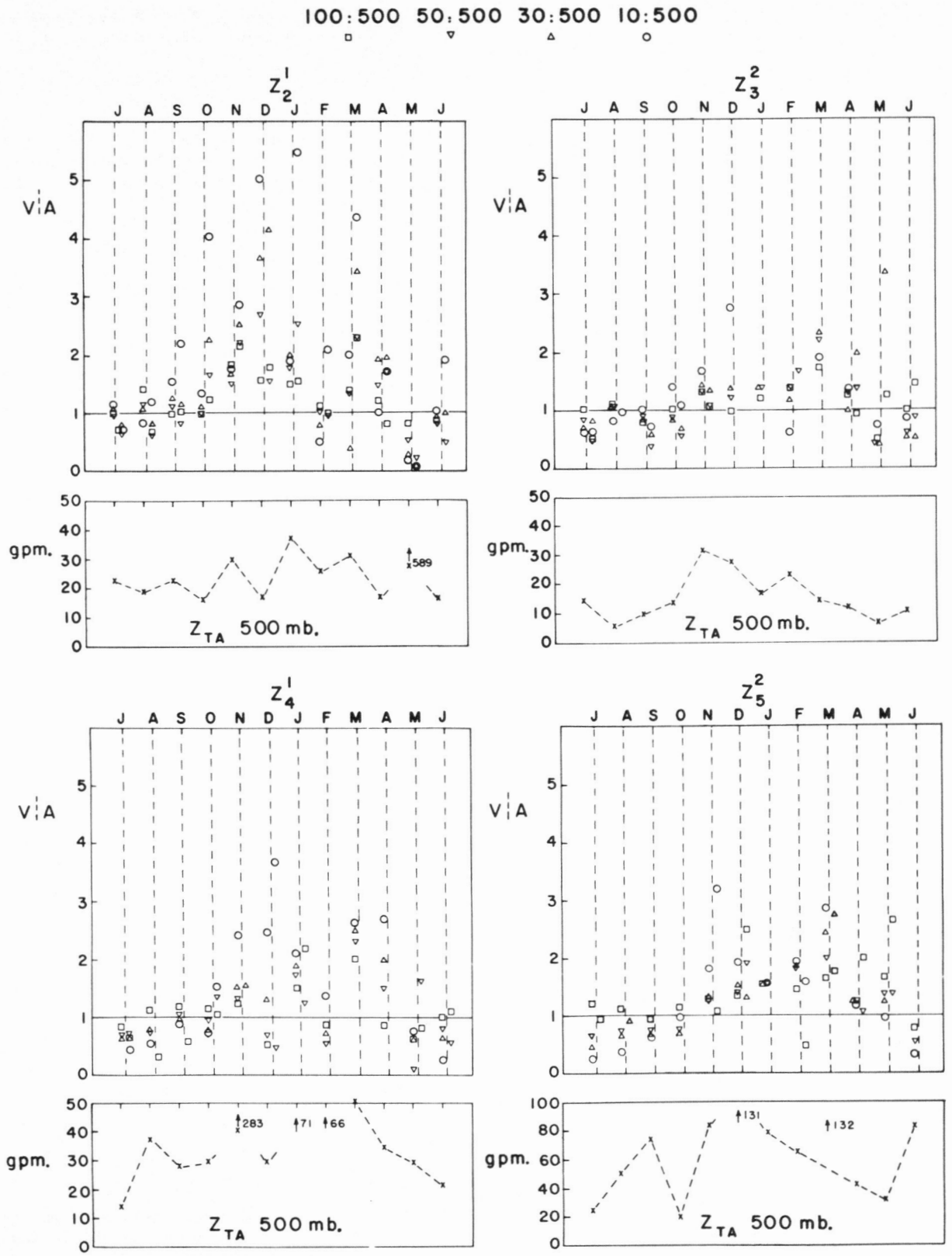

FIGURE 10.—Estimated ratios of amplitudes of TPSW at 100, 50, 30, and 10 mb. relative to amplitude at 500 mb., July 1964–June 1965. Under each month, ratio estimated from vertical regression, Z_{T_V}, is plotted on the left; ratio of amplitudes from autoregression, Z_{T_A}, is plotted on right. The estimated amplitude at 500 mb. is plotted in lower part of each figure.

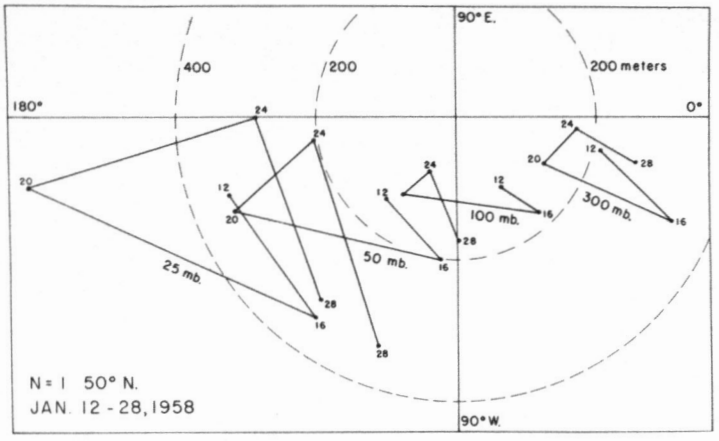

FIGURE 11.—Polar representation of N=1 at 50° N., 300 mb.–25 mb., during January 1958 from Muench [16]. Data are 4 days apart; numbers are dates in January.

The average tilt of the coherent fluctuations toward the west with increasing height is in the same direction as, but much smaller in magnitude than, that observed for the quasi-stationary waves. As for the quasi-stationary waves, as discussed by several authors (e.g. Boville [2]), the westward tilt implies some forcing from below through the associated vertical velocity fields.

The possibility that the TPSW, or simply tropospheric-stratospheric relations of the same general nature, may be an important aspect of the "stratospheric-warming" phenomenon is of interest. Labitzke [14] has pointed out tropospheric "blocking" patterns associated with stratospheric warming episodes. There were no conspicuous large-scale warming events during the late winter of 1964–65, but considerable data on the large-scale stratospheric-warming event of January 1958 are available.

Muench's [16] harmonic analyses for wave-number 1 at 50°N. are replotted in figure 11. It is apparent that approximately congruent changes of the TPSW kind, of the same phase and increasing in magnitude with increasing height, occurred simultaneously at all levels from 300 mb. to 25 mb. during January 1959. These data also show the westward tilt, or leading, with increasing height. Sawyer's [19] data for wave-number 2, when plotted in the same way, show similar correlation of changes in the troposphere and stratosphere after the middle of the month; in this case the correlated changes are evident when phase and amplitude are considered separately, as pointed out by Sawyer. These data support Boville's [2] conclusion that the large-amplitude, vortex-disrupting changes characteristic of the late winter stratosphere may at least sometimes be in response to tropospheric disturbances.

ACKNOWLEDGMENTS

The help of Miss Margaret Drake, NCAR, is gratefully acknowledged. The work was also supported by a grant of computing time by NCAR.

REFERENCES

1. T. W. Anderson, *An Introduction to Multivariate Statistical Analysis*, John Wiley and Sons, New York, 1958, 374 pp.
2. B. W. Boville, "Planetary Waves in the Stratosphere and Their Upward Propagation," *Space Research*, vol. 7, 1966, pp. 20–29.
3. R. Byron-Scott, "A Stratospheric General Circulation Experiment," *Publication in Meteorology*, No. 87, McGill University, Montreal, Apr. 1967, p. 201.
4. J. G. Charney and P. G. Drazin, "Propagation of Planetary-Scale Disturbances From the Lower Into the Upper Atmosphere," *Journal of Geophysical Research*, vol. 66, No. 1, Jan. 1961, pp. 83–110.
5. G. P. Cressman, "Barotropic Divergence and Very Long Atmospheric Waves," *Monthly Weather Review*, vol. 86, No. 8, Aug. 1958, pp. 293–297.
6. R. J. Deland, "Some Observations of the Behavior of Spherical Harmonic Waves," *Monthly Weather Review*, vol. 93, No. 5, May 1965, pp. 307–312.
7. R. J. Deland and Y.-J. Lin, "On the Movement and Prediction of Traveling Planetary-Scale Waves," *Monthly Weather Review*, vol. 95, No. 1, Jan. 1967, pp. 21–31.
8. E. Eliasen and B. Machenhauer, "A Study of the Fluctuations of the Atmospheric Planetary Flow Patterns," *Tellus*, vol. 17, No. 2, May 1965, pp. 220–238.
9. T. H. Ellison, "On the Correlation of Vectors," *Quarterly Journal of the Royal Meteorological Society*, vol. 80, No. 343, Jan. 1955, pp. 93–96.
10. F. G. Finger, H. M. Woolf, and C. E. Anderson, "A Method For Objective Analysis of Stratospheric Constant-Pressure Charts," *Monthly Weather Review*, vol. 93, No. 10, Oct. 1965, pp. 619–638.
11. F. K. Hare and B. W. Boville, "The Polar Circulations," Chapter III of "The Circulation in the Stratosphere, Mesosphere, and Lower Thermosphere," *W. M. O. Technical Note*, No. 70, 1965, p. 206.
12. B. Haurwitz, "The Motion of Atmospheric Disturbances on a Spherical Earth," *Journal of Marine Research*, vol. 3, No. 3, Dec. 1940, pp. 254–267.
13. P. R. Julian and K. B. Labitzke, "A Study of Atmospheric Energetics During the January-February 1963 Stratospheric Warming," *Journal of Atmospheric Sciences*, vol. 22, No. 6, Nov. 1965, pp. 597–610.
14. K. Labitzke, "On the Mutual Relation Between Stratosphere and Troposphere During Periods of Stratospheric Warmings in Winter," *Journal of Applied Meteorology*, vol. 4, No. 1, Feb. 1965, pp. 91–99.
15. N. E. LaSeur, "On the Asymmetry of the Middle-Latitude Circumpolar Current," *Journal of Meteorology*, vol. 11, No. 1, Feb. 1954, pp. 43–57.
16. H. S. Muench, "On the Dynamics of the Wintertime Stratospheric Circulation," *Journal of the Atmospheric Sciences*, vol. 22, No. 4, July 1965, pp. 349–360.
17. G. P. Platzman, "The Analytical Dynamics of the Spectral Vorticity Equation," *Journal of the Atmospheric Sciences*, vol. 19, No. 4, July 1962, pp. 313–328.
18. C.-G. Rossby and others, "Relations Between Variations in the Intensity of the Zonal Circulation of the Atmosphere and the Displacements of the Semi-Permanent Centers of Action," *Journal of Marine Reserach*, vol. 2, No. 1, June 1939, pp. 38–55.
19. J. S. Sawyer, "The Dynamical Problems of the Lower Stratosphere," *Quarterly Journal of the Royal Meteorological Society*, vol. 91, No. 390, Oct. 1965, pp. 407–416.
20. F. G. Shuman, J. D. Stackpole, and L. W. Vanderman, *A Multi-Level Primitive Equation Model Suitable for Operational Numerical Weather Prediction* (a collection of three papers) Environmental Science Services Administration, Nov. 1965, 22 pp. [Obtainable from National Meteorological Center, Weather Bureau, ESSA, Washington, D.C.]

[Received April 26, 1967; revised September 11, 1967]